

Metabolomic Profile of Human Myocardial Ischemia by Nuclear Magnetic Resonance Spectroscopy of Peripheral Blood Serum

A Translational Study Based on Transient Coronary Occlusion Models

Vicente Bodi, MD,* Juan Sanchis, MD,* Jose M. Morales, BSc,† Vannina G. Marrachelli, PhD,* Julio Nunez, MD,* Maria J. Forteza, BSc,* Fabian Chaustre, BSc,* Cristina Gomez, BSc,* Luis Mainar, MD,* Gema Minana, MD,* Eva Rumiz, MD,* Oliver Husser, MD,* Inmaculada Noguera, PhD,† Ana Diaz, PhD,† David Moratal, PhD,‡ Arturo Carratala, MD,§ Xavier Bosch, MD,|| Angel Llacer, MD,* Francisco J. Chorro, MD,* Juan R. Viña, MD, PhD,¶# Daniel Monleon, PhD#

Valencia and Barcelona, Spain

Objectives

The aim of this study was to investigate the metabolomic profile of acute myocardial ischemia (MIS) using nuclear magnetic resonance spectroscopy of peripheral blood serum of swine and patients undergoing angioplasty balloon-induced transient coronary occlusion.

Background

Biochemical detection of MIS is a major challenge. The validation of novel biosignatures is of utmost importance.

Methods

High-resolution nuclear magnetic resonance spectroscopy was used to profile 32 blood serum metabolites obtained (before and after controlled ischemia) from swine (n = 9) and patients (n = 20) undergoing transitory MIS in the setting of planned coronary angioplasty. Additionally, blood serum of control patients (n = 10) was sequentially profiled. Preliminary clinical validation of the developed metabolomic biosignature was undertaken in patients with spontaneous acute chest pain (n = 30).

Results

Striking differences were detected in the blood profiles of swine and patients immediately after MIS. MIS induced early increases (10 min) of circulating glucose, lactate, glutamine, glycine, glycerol, phenylalanine, tyrosine, and phosphoethanolamine; decreases in choline-containing compounds and triacylglycerols; and a change in the pattern of total, esterified, and nonesterified fatty acids. Creatine increased 2 h after ischemia. Using multivariate analyses, a biosignature was developed that accurately detected patients with MIS both in the setting of angioplasty-related MIS (area under the curve 0.94) and in patients with acute chest pain (negative predictive value 95%).

Conclusions

This study reports, to the authors' knowledge, the first metabolic biosignature of acute MIS developed under highly controlled coronary flow restriction. Metabolic profiling of blood plasma appears to be a promising approach for the early detection of MIS in patients. (J Am Coll Cardiol 2012;59:1629–41) © 2012 by the American College of Cardiology Foundation

Decision making in patients with suspected acute myocardial ischemia (MIS), especially in those with normal results in the current standard of care based on electrocardiographic results and troponin levels, is among the most challenging tasks doctors face in emergency departments (1). In this scenario, biomarkers or biosignatures with the ability to

reliably discriminate ischemic from nonischemic patients would be highly appreciated, and they could have important clinical implications in daily practice to reduce the use of

See page 1642

From the *Cardiology Department, Hospital Clínico Universitario-INCLIVA, Universidad de Valencia, Valencia, Spain; †Unidad Central de Investigación en Medicina, Universidad de Valencia, Valencia, Spain; ‡Centro de Biomateriales e Ingeniería Tisular, Universidad Politécnica de Valencia, Valencia, Spain; §Department of Clinical Analyses, Hospital Clínico Universitario-INCLIVA, Valencia, Spain; ||Cardiology Department, Hospital Clínic, IDIBAPS, Universidad de Barcelona, Barcelona, Spain; ¶Department of Biochemistry and Molecular Biology, Facultad de Medicina, Universidad de Valencia, Valencia, Spain; and the #Fundación Investigación, Hospital Clínico Universitario-INCLIVA, Valencia, Spain. The present study was

supported by Instituto de Salud Carlos III (PI 11/02323 and Heracles grants to Dr. Bodi), Fundación Gent per Gent (to Drs. Bodi and Monleon), the Ministry of Science and Innovation of Spain (grant SAF2008-00270 to Dr. Monleon), and Generalitat Valenciana (grant GVASAN AP014/2009 to Dr. Monleon and grant PROMETEO2010-075 to Dr. Viña). Dr. Monleon gratefully acknowledges a 2006 Ramon y Cajal contract from the Ministry of Education of Spain. All other authors have reported that they have no relationships relevant to the contents of this paper to disclose.

Manuscript received August 4, 2011; accepted September 25, 2011.

Abbreviations and Acronyms

FA	= fatty acid
MIS	= myocardial ischemia
NMR	= nuclear magnetic resonance
PCA	= principal component analysis
PLS-DA	= projection to latent structures for discriminant analysis

unnecessary resources in the workup of patients and to avoid inappropriate discharges. Several studies have reported potential biomarkers of MIS, although so far, none has reached routine practice, because of insufficient accuracy (2–4).

Altered cardiac metabolism is the primary consequence of MIS. Metabolomics permits a quantitative measurement of the multiparametric metabolic re-

sponses of living systems to pathophysiological stimuli by simultaneously examining dynamic changes in hundreds of low-molecular weight metabolites in tissues or biofluids (5). However, human metabolomics studies are at risk for potential clinical confounders such as interindividual variability, diet, drug effects, age, sex, and comorbidities. Serial sampling performed in patients both before and after a controlled perturbation may circumvent these problems, allowing each patient to serve as his or her own biological control (5).

High-resolution nuclear magnetic resonance (NMR) spectroscopy combined with advanced multivariate analyses methodologies poses several advantages over classical biochemical assays. First, it represents a powerful, reproducible, and inexpensive technique for investigating the metabolome in the area of disease diagnosis without extensive sample preparation. Second, simultaneous measurements of changes in multiple metabolic parameters are detectable in as little as 20 μ l (just a couple of drops) of peripheral blood plasma. And last but not least, NMR spectra provide information not only about the amounts of certain metabolites but also about their physicochemical status (6–8).

Transient angioplasty balloon-induced coronary occlusion is ideally suited for metabolomic studies. Not only does it allow a highly controlled model of MIS (9), but it also avoids the confusing effects of metabolic responses of large muscle groups. The latter inevitably occurs in exercise-induced ischemia (7) and could potentially interfere with the interpretation of the effects of MIS on the peripheral blood plasma metabolomic profile.

The aim of the present study was to develop a metabolic profile of acute MIS in peripheral blood serum. For this purpose, we used, in swine and patients, highly controlled models of MIS based on transient angioplasty balloon-induced coronary occlusion. The role of metabolomics to detect MIS in such a controlled fashion has not been previously evaluated. A preliminary clinical validation of the developed biosignature was carried out in patients with spontaneous acute chest pain and normal electrocardiographic results and troponin values.

Methods

Chemometric analysis of high-resolution NMR spectroscopic findings for blood serum metabolic profiling was used throughout. The 3 steps of the present study are detailed as follows and in Figure 1.

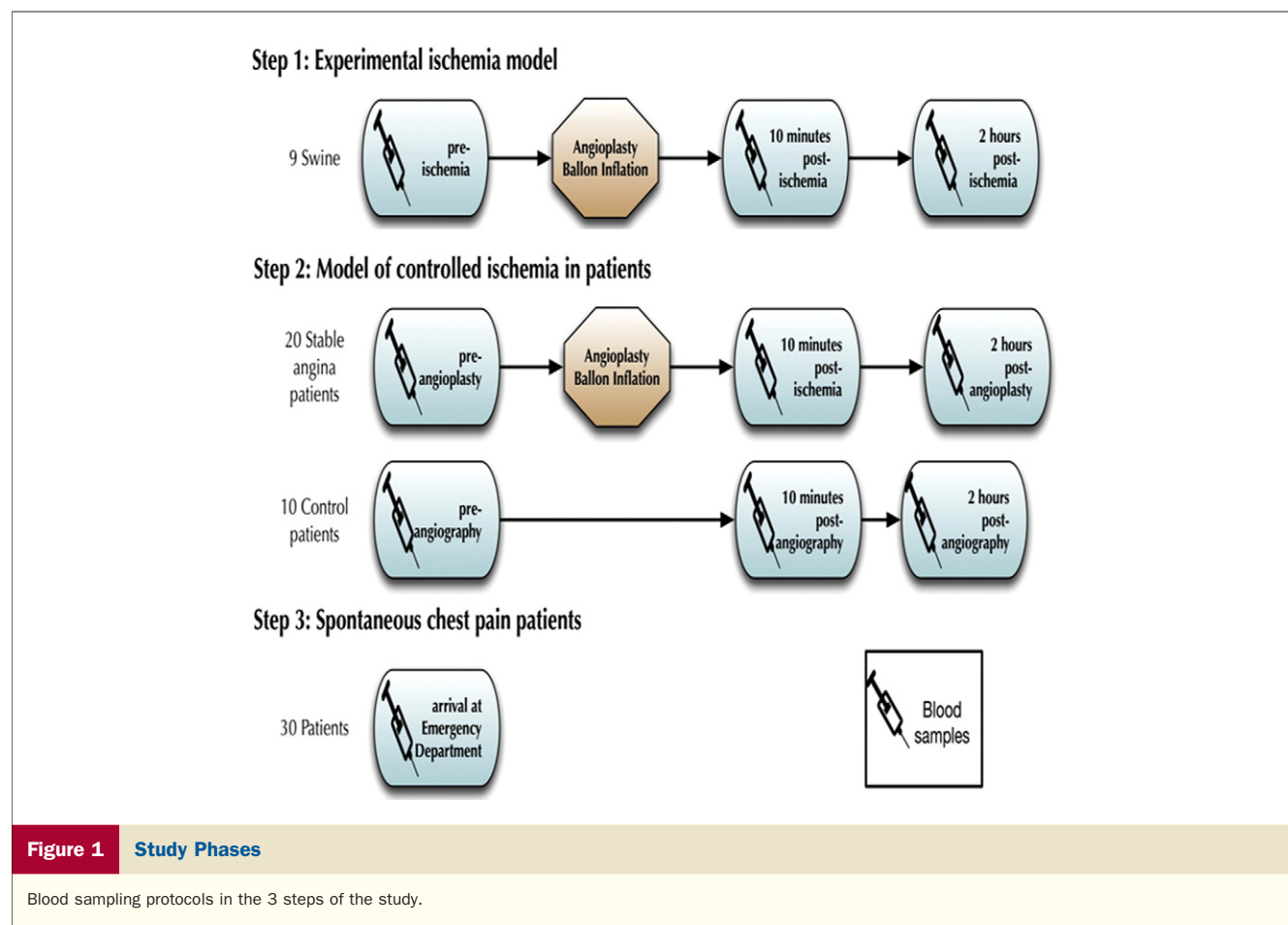
Experimental study on animal models. After fasting for at least 12 h, 9 juvenile domestic female pigs weighing 25 to 30 kg were sedated and anesthetized, and transient angioplasty balloon-induced MIS in the proximal left anterior descending coronary artery was induced, as we have previously described (10). Coronary artery occlusion was confirmed by contrast injection and by electrocardiographic ST-segment deviation. After 5 min, the balloon was deflated, and restoration of normal coronary flow was documented by angiography.

Once diagnostic angiography had been performed, blood samples were drawn before and 10 and 120 min after ischemia. Samples were prepared and frozen for subsequent analyses. The animals were allowed to recover. For all metabolomic analyses, the state before ischemia was used as the own control in each experiment. No deaths, significant complications, coronary dissection, or closure was detected.

The study was approved by the Animal Care and Use Committee of the University of Valencia and conformed to the Guide for the Care and Use of Laboratory Animals published by the U.S. National Institutes of Health (NIH Publication No. 85-23, revised 1996).

Controlled model of ischemia in patients. A group of 21 ambulatory patients without acute coronary syndromes scheduled to undergo percutaneous coronary intervention for stable angina were enrolled. Patients were treated with heparin (100 U/kg). Medical treatment was not stopped and was left at the discretion of the attending cardiologists. Patients fasted for 12 h before and after the procedure. A 6-F sheath was introduced into the left radial artery to engage the culprit coronary artery. Appropriate catheters and angioplasty wires were used. Ischemia was induced by inflating the appropriate balloon in each case. At least 1 min of uninterrupted total coronary occlusion was confirmed in all patients by contrast injection and ST-segment deviation. Stents were successfully implanted in all patients. No deaths or significant complications were detected. Troponin I (Dade Behring, Newark, Delaware) was serially measured at 6 and 12 h after angioplasty. One patient was excluded because of an asymptomatic post-procedural troponin I increase. Accordingly, the study group comprised 20 patients. Once diagnostic angiography had been carried out, peripheral blood samples for metabolomic analyses were drawn before and 10 and 120 min after angioplasty. Samples were prepared and frozen for subsequent analyses.

A control group made up of 10 patients studied with coronary angiography but with normal coronary arteries was included. The same protocol applied in patients was used in controls. Blood samples for metabolomic analyses were



drawn immediately, 10 min, and 120 min after angiography. The study protocol was approved by an ethics committee, and all subjects gave written informed consent.

Study group with spontaneous chest pain. We tested the accuracy of the metabolomic biosignature developed from blood samples obtained 10 min after angioplasty-induced MIS to predict a final diagnosis of MIS in blood drawn on arrival at the emergency department in patients with spontaneous acute chest pain and normal electrocardiographic results and troponin values. Forty-six consecutive patients entering our emergency department at most 4 h after acute chest pain onset were enrolled. Patients with ST-segment deviation at admission ($n = 7$) and/or troponin I elevation in any determination ($n = 9$) were excluded. Accordingly, the final study group comprised 30 patients. As previously defined by our group (1), a final diagnosis of MIS was established in the case of abnormal noninvasive stress test results (either exercise testing or stress perfusion cardiac magnetic resonance) and/or abnormal coronary angiographic findings. A final diagnosis of MIS was established in 10 of 30 patients. The study protocol was approved by an ethics committee, and all subjects gave written informed consent.

NMR spectroscopy. Two microliters of D_2O were added to 20 μl of blood serum, and an aliquot of 20 μl was

taken and placed in a 1-mm NMR tube. Hydrogen-1 NMR spectra were recorded using a Bruker Avance DRX 600 spectrometer (Bruker GmbH, Rheinstetten, Germany). Samples were measured at 37°C. Reproducibility of NMR spectroscopy was tested by superposition of normalized spectra of blood serum before and immediately after ischemia (Online Fig. 1). Signals belonging to selected metabolites (Online Table 1) were integrated and quantified using semiautomated in-house MATLAB 6.5 (The MathWorks Inc., Natick, Massachusetts) peak-fitting routines. Principal component analysis (PCA) and projection to latent structures for discriminant analysis (PLS-DA) were applied to NMR spectral datasets. Results were cross-validated using the leave-one-out approach. Additional information about NMR data processing and the construction and validation of multivariable metabolomic models is available in the Online Appendix.

Statistical analysis. Metabolite levels are expressed as mean \pm SD in tables and as box plots in figures. In box plots, boxes denote interquartile ranges, lines denote medians, and whiskers denote the 10th and 90th percentiles.

Several comparisons were performed on the data. First, we compared, both in swine and in humans, the metabolic profiles before and after controlled ischemia (Figs. 2 and 3,

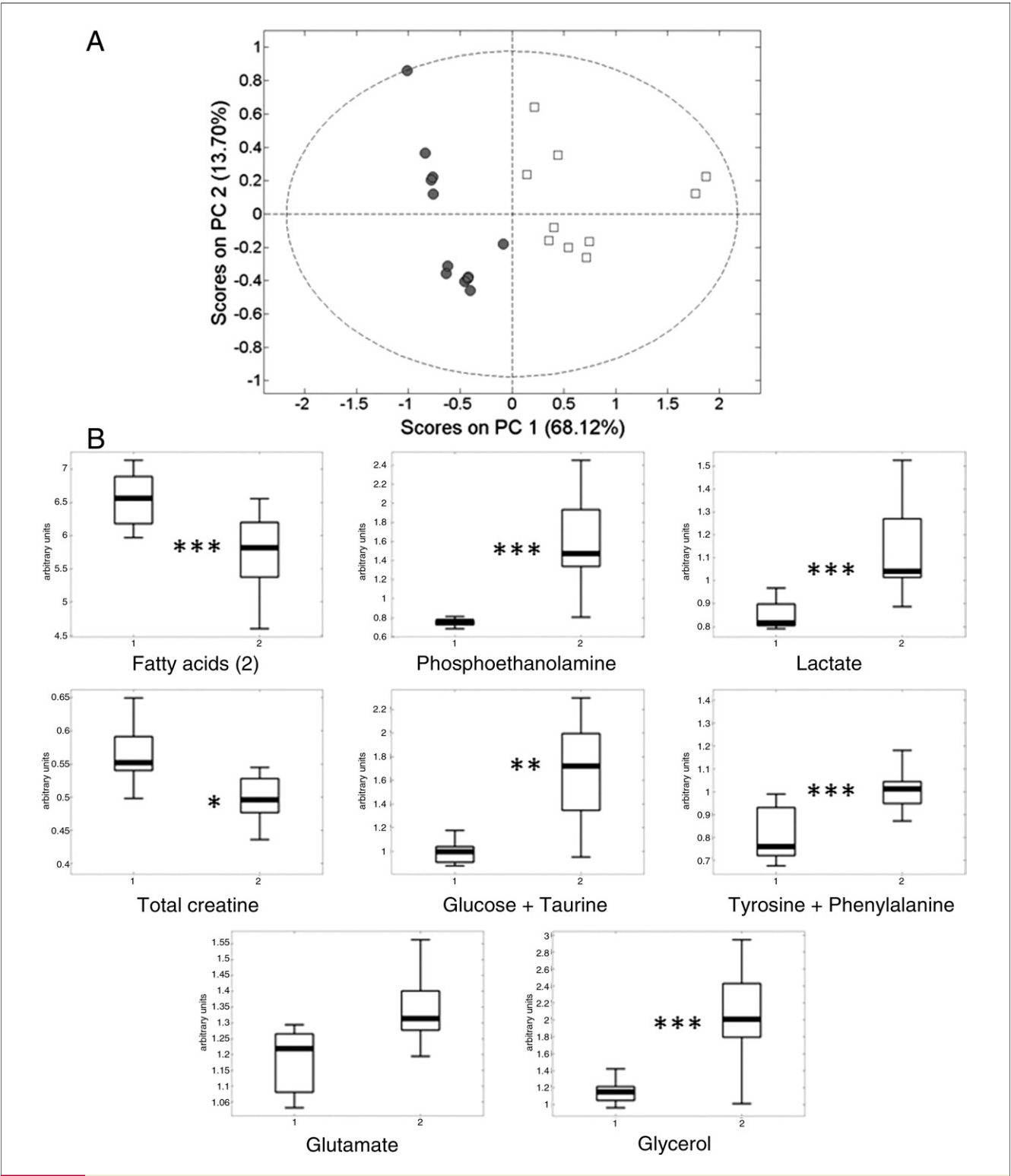


Figure 2 Metabolic Analysis in the Experimental Model

Principal component (PC) analysis and metabolic quantification of selected metabolites in the experimental model. **(A)** Score plot of the first (PC1) and second (PC2) PCs (horizontal and vertical axes, respectively) from principal component analysis of the nuclear magnetic resonance spectra of blood serum in the experimental model before (gray circles) and immediately after (open squares) ischemia. **(B)** Box plots showing metabolite changes in blood serum before (box on the left) and immediately after (box on the right) ischemia in the experimental model. Boxes denote interquartile ranges, lines denote medians, and whiskers denote 10th and 90th percentiles. This set of metabolites is representative of most of the processes affected by myocardial ischemia. Levels are expressed as area of the metabolite of interest divided with respect total aliphatic spectral area. * $p < 0.02$; ** $p < 0.01$; *** $p < 0.001$.

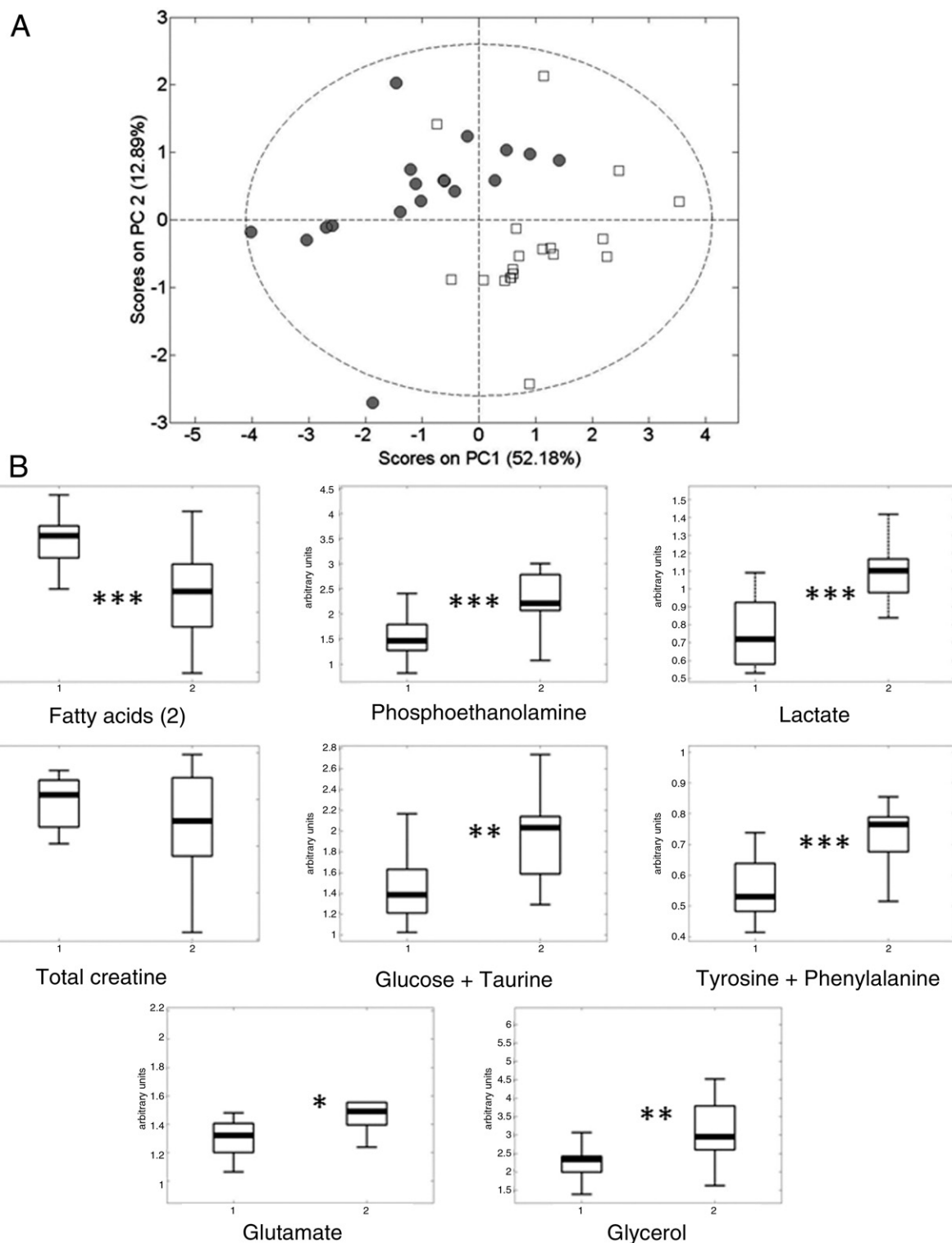


Figure 3 Metabolic Analysis in Patients Undergoing Angioplasty-Induced Ischemia

Principal component analysis (PCA) and metabolic quantification of selected metabolites in patients undergoing angioplasty-induced ischemia. **(A)** PCA score plot of blood serum nuclear magnetic resonance spectra in patients before (**gray circles**) and immediately after (**open squares**) angioplasty-induced ischemia. **(B)** Box plots showing representative metabolite changes in blood serum before (**box on the left**) and immediately after (**box on the right**) angioplasty-induced ischemia in patients. The **boxes and whiskers** represent the same as in Figure 2. Levels are expressed as area of the metabolite of interest divided with respect total aliphatic spectral area. * $p < 0.02$; ** $p < 0.01$; *** $p < 0.001$.

Table 1 Metabolite Levels in the Experimental Model

Metabolite Dominant in the Spectral Region	Mean Spectral Intensity (Arbitrary Units)				
	Before Ischemia	10 Min After Intervention	p Value*	2 h After Intervention	p Value*
Cholesterol	3.69 ± 0.24	3.28 ± 0.32	0.003	3.44 ± 0.29	0.0404
Triglycerides	6.56 ± 0.37	5.76 ± 0.54	0.0005	6.20 ± 0.43	0.0458
Leucine	2.79 ± 0.10	2.63 ± 0.16	0.009	2.71 ± 0.16	0.1755
Isoleucine	0.89 ± 0.03	0.82 ± 0.04	0.0006	0.84 ± 0.05	0.0114
Valine	0.77 ± 0.02	0.69 ± 0.04	0.00002	0.71 ± 0.04	0.0001
3-hydroxybutyrate	1.84 ± 0.22	1.54 ± 0.16	0.001	1.64 ± 0.12	0.0144
FAs†	8.57 ± 1.25	7.27 ± 0.95	0.012	9.00 ± 1.01	0.3909
Alanine (overlapped)	1.11 ± 0.03	1.00 ± 0.07	0.00006	1.02 ± 0.05	0.0000
FAs‡	1.48 ± 0.06	1.33 ± 0.08	0.00006	1.40 ± 0.07	0.0097
Acetate	1.66 ± 0.08	2.54 ± 0.54	0.00002	2.14 ± 0.34	0.0001
Unsaturated FAs	1.95 ± 0.08	1.82 ± 0.10	0.004	1.95 ± 0.16	0.9908
Glycoproteins (acetyls)	1.67 ± 0.08	1.54 ± 0.13	0.008	1.57 ± 0.14	0.0577
FAs§	1.51 ± 0.06	1.36 ± 0.08	0.00009	1.47 ± 0.15	0.3791
Glutathione	1.39 ± 0.10	1.32 ± 0.08	0.114	1.33 ± 0.13	0.2785
Glutamate	0.72 ± 0.05	0.69 ± 0.03	0.0922	0.69 ± 0.06	0.1901
Glutamine	0.73 ± 0.07	0.94 ± 0.14	0.0002	0.81 ± 0.12	0.0723
Polyunsaturated FAs	1.76 ± 0.06	1.58 ± 0.18	0.00410	1.65 ± 0.10	0.0043
Asparagine	0.61 ± 0.03	0.55 ± 0.07	0.0121	0.54 ± 0.04	0.0001
Albumine lysyl	0.76 ± 0.04	0.69 ± 0.08	0.0137	0.68 ± 0.04	0.0001
Albumine lysyl	0.36 ± 0.01	0.32 ± 0.03	0.0007	0.33 ± 0.02	0.0001
Creatine	0.56 ± 0.04	0.51 ± 0.06	0.0162	0.53 ± 0.06	0.1019
Choline	0.32 ± 0.04	0.28 ± 0.04	0.0174	0.29 ± 0.03	0.0424
Phosphocholine	0.36 ± 0.08	0.29 ± 0.06	0.0238	0.33 ± 0.05	0.2341
Glycerophosphocholine	0.32 ± 0.10	0.34 ± 0.11	0.774	0.39 ± 0.12	0.1597
Taurine	1.47 ± 0.11	1.31 ± 0.16	0.0115	1.34 ± 0.12	0.0218
Proline	0.38 ± 0.03	0.36 ± 0.07	0.424	0.34 ± 0.05	0.0266
Glucose	0.68 ± 0.09	1.03 ± 0.22	0.00008	0.85 ± 0.18	0.0116
Glycine	0.17 ± 0.02	0.24 ± 0.05	0.00014	0.21 ± 0.04	0.0057
Glycerol	1.62 ± 0.19	3.25 ± 0.98	0.00002	2.47 ± 0.64	0.0004
Glucose + taurine	1.01 ± 0.12	1.68 ± 0.38	0.00001	1.28 ± 0.22	0.0018
Tyrosine + phenylalanine	0.80 ± 0.11	1.02 ± 0.15	0.0009	0.92 ± 0.18	0.0971
Phosphoethanolamine	0.77 ± 0.08	1.61 ± 0.49	0.00001	1.21 ± 0.34	0.0004
Lactate	0.85 ± 0.06	1.13 ± 0.20	0.0001	1.00 ± 0.18	0.0147

Values are mean ± SD. *p values versus baseline. †CH₃ groups in FAs. ‡CH₃ groups close to a CO group (CH₃-CO-) in FAs. §CH₃ groups close to a double bond (CH₃-CH=CH-) in FAs. ||Different spectral positions for the same group in the same molecules.

FA = fatty acid.

Tables 1 and 2). Second, we compared the metabolic profile of the blood samples obtained 10 min after the procedure in patients and controls (Fig. 4). Post-procedural time changes of selected metabolites were also assessed (Fig. 5). Finally, we compared the metabolic profile in patients with spontaneous acute chest pain with and without MIS in the blood sample obtained on arrival at the emergency department (Table 3).

Continuous data were compared using the Student *t* test or Mann-Whitney 2-tailed test as appropriate. Categorical data comparisons were performed using the chi-square test and the Fisher exact test if indicated. Receiver-operating characteristic curve analyses were used to test the accuracy of the PLS-DA discrimination model (Figs. 6 and 7). Statistical significance was considered for p values <0.05. SPSS version 15.0 (SPSS, Inc., Chicago, Illinois) was used throughout. Additional

information regarding the statistical analysis can be found in the Online Appendix.

Results

Experimental study. MIS by balloon inflation induced clear, reproducible, and dramatic metabolic changes in swine. The PCA score plot of the global metabolic profile of swine serum before and immediately after ischemia demonstrates these changes (Fig. 2A). Our results revealed that MIS induced immediate increases, among others, in circulating glucose, lactate, glutamine, glycine, glycerol, phenylalanine, tyrosine, and phosphoethanolamine and decreases in total NMR visible fatty acids (FAs) (nonesterified and esterified), polyunsaturated FAs, triglycerides, choline-containing compounds, and 3-hydroxybutyrate (Table 1). Two hours after intervention, many of these changes per-

Table 2 Metabolite Levels in Angiographic Controls and in Angioplasty-Induced Ischemia Patients

Metabolite Dominant in the Spectral Region	Mean Spectral Intensity (Arbitrary Units)								
	Before Ischemia			10 Min After Intervention			2 h After Intervention		
	Angiographic Controls (n = 10)	Angioplasty-Induced Ischemia (n = 20)	p Value*	Angiographic Controls (n = 10)	Angioplasty-Induced Ischemia (n = 20)	p Value*	Angiographic Controls (n = 10)	Angioplasty-Induced Ischemia (n = 20)	p value*
Cholesterol	2.84 ± 0.62	2.67 ± 0.33	0.37	2.65 ± 0.67	2.43 ± 0.60	0.405	3.11 ± 0.07	2.61 ± 0.54	0.103
Triglycerides	8.65 ± 0.69	8.18 ± 0.41	0.04	8.45 ± 0.50	7.33 ± 0.71	0.0004	8.93 ± 0.47	8.07 ± 0.27	0.0002
Leucine	2.68 ± 0.24	2.65 ± 0.11	0.62	2.68 ± 0.19	2.44 ± 0.27	0.024	2.69 ± 0.15	2.69 ± 0.18	0.967
Isoleucine	0.86 ± 0.07	0.85 ± 0.03	0.51	0.87 ± 0.07	0.77 ± 0.08	0.024	0.88 ± 0.06	0.85 ± 0.06	0.496
Valine	0.68 ± 0.07	0.67 ± 0.03	0.68	0.67 ± 0.07	0.62 ± 0.08	0.088	0.70 ± 0.05	0.68 ± 0.06	0.619
3-hydroxybutyrate	1.90 ± 0.27	1.82 ± 0.13	0.35	1.89 ± 0.32	1.69 ± 0.27	0.121	2.76 ± 1.22	1.87 ± 0.59	0.063
FAs†	15.86 ± 3.44	14.84 ± 1.48	0.30	15.04 ± 2.56	13.02 ± 2.08	0.042	17.39 ± 2.51	15.76 ± 2.37	0.260
Alanine (overlapped)	1.07 ± 0.09	1.10 ± 0.05	0.39	1.12 ± 0.07	1.02 ± 0.09	0.011	1.13 ± 0.08	1.13 ± 0.10	0.963
FAs‡	1.65 ± 0.37	1.63 ± 0.15	0.86	1.62 ± 0.23	1.45 ± 0.22	0.094	1.79 ± 0.17	1.80 ± 0.28	0.948
Acetate	2.96 ± 1.07	3.10 ± 0.63	0.68	2.94 ± 0.52	4.16 ± 1.02	0.003	1.81 ± 0.13	2.42 ± 0.68	0.108
Unsaturated FAs	2.48 ± 0.45	2.42 ± 0.18	0.63	2.44 ± 0.25	2.19 ± 0.23	0.016	2.79 ± 0.30	2.54 ± 0.22	0.089
Glycoproteins (acetyls)	1.87 ± 0.27	1.89 ± 0.12	0.79	1.88 ± 0.14	1.76 ± 0.17	0.086	1.92 ± 0.16	2.02 ± 0.16	0.260
FAs§	1.50 ± 0.41	1.52 ± 0.17	0.82	1.49 ± 0.24	1.40 ± 0.23	0.336	1.76 ± 0.21	1.75 ± 0.31	0.966
Glutathione	1.15 ± 0.16	1.20 ± 0.08	0.28	1.22 ± 0.14	1.14 ± 0.13	0.166	1.20 ± 0.18	1.28 ± 0.10	0.274
Glutamate	0.52 ± 0.07	0.56 ± 0.04	0.11	0.56 ± 0.06	0.53 ± 0.05	0.212	0.56 ± 0.09	0.59 ± 0.07	0.411
Glutamine	1.02 ± 0.22	1.09 ± 0.17	0.33	1.07 ± 0.17	1.38 ± 0.26	0.003	0.71 ± 0.11	0.96 ± 0.19	0.028
Polyunsaturated FAs	1.80 ± 0.32	1.84 ± 0.17	0.72	1.90 ± 0.13	1.67 ± 0.22	0.011	1.95 ± 0.08	1.88 ± 0.22	0.579
Asparagine	0.49 ± 0.06	0.52 ± 0.03	0.07	0.53 ± 0.06	0.49 ± 0.05	0.168	0.52 ± 0.08	0.55 ± 0.05	0.405
Albumine lysyl	0.66 ± 0.07	0.69 ± 0.04	0.18	0.68 ± 0.08	0.64 ± 0.07	0.186	0.66 ± 0.10	0.71 ± 0.06	0.322
Albumine lysyl	0.32 ± 0.03	0.33 ± 0.02	0.11	0.33 ± 0.03	0.31 ± 0.03	0.062	0.32 ± 0.03	0.33 ± 0.04	0.674
Creatine	0.47 ± 0.05	0.50 ± 0.03	0.06	0.49 ± 0.07	0.47 ± 0.05	0.417	0.49 ± 0.08	0.64 ± 0.05	0.0187
Choline	0.25 ± 0.06	0.26 ± 0.03	0.54	0.27 ± 0.08	0.25 ± 0.07	0.397	0.28 ± 0.08	0.24 ± 0.06	0.265
Phosphocholine	0.34 ± 0.08	0.34 ± 0.04	0.93	0.38 ± 0.10	0.33 ± 0.09	0.255	0.34 ± 0.08	0.31 ± 0.08	0.566
Glycerophosphocholine	0.44 ± 0.09	0.42 ± 0.05	0.53	0.45 ± 0.10	0.40 ± 0.08	0.143	0.42 ± 0.08	0.40 ± 0.09	0.726
Taurine	1.34 ± 0.25	1.32 ± 0.13	0.75	1.35 ± 0.24	1.20 ± 0.21	0.140	1.29 ± 0.23	1.39 ± 0.18	0.389
Proline	0.16 ± 0.04	0.18 ± 0.03	0.10	0.18 ± 0.03	0.17 ± 0.02	0.350	0.18 ± 0.04	0.20 ± 0.03	0.337
Glucose	1.10 ± 0.46	1.20 ± 0.22	0.46	1.12 ± 0.21	1.64 ± 0.42	0.002	0.64 ± 0.02	1.04 ± 0.27	0.011
Glycine	0.22 ± 0.09	0.24 ± 0.04	0.50	0.21 ± 0.03	0.32 ± 0.10	0.006	0.15 ± 0.01	0.20 ± 0.04	0.027
Glycerol	3.20 ± 1.55	3.47 ± 0.93	0.59	3.23 ± 0.77	5.06 ± 1.43	0.002	1.45 ± 0.24	2.58 ± 0.91	0.033
Glucose + taurine	1.27 ± 0.46	1.46 ± 0.57	0.26	1.32 ± 0.31	1.93 ± 0.36	0.002	0.87 ± 0.04	1.32 ± 0.25	0.029
Tyrosine + phenylalanine	0.44 ± 0.25	0.55 ± 0.09	0.13	0.51 ± 0.09	0.73 ± 0.11	0.00004	0.41 ± 0.06	0.54 ± 0.07	0.0072
Phosphoethanolamine	1.29 ± 0.74	1.49 ± 0.46	0.39	1.32 ± 0.28	2.37 ± 0.71	0.0004	0.64 ± 0.08	1.13 ± 0.38	0.0266
Lactate	0.57 ± 0.40	0.75 ± 0.17	0.13	0.66 ± 0.14	1.07 ± 0.21	0.00002	0.53 ± 0.05	0.72 ± 0.10	0.002

Values are mean ± SD. *p values versus angiographic controls. †CH₃ groups in FAs. ‡CH₃ groups close to a CO group (CH₃-CO-) in FAs. §CH₃ groups close to a double bond (CH₃-CH=CH-) in FAs. ||Different spectral positions for the same group in the same molecules. FA = fatty acid.

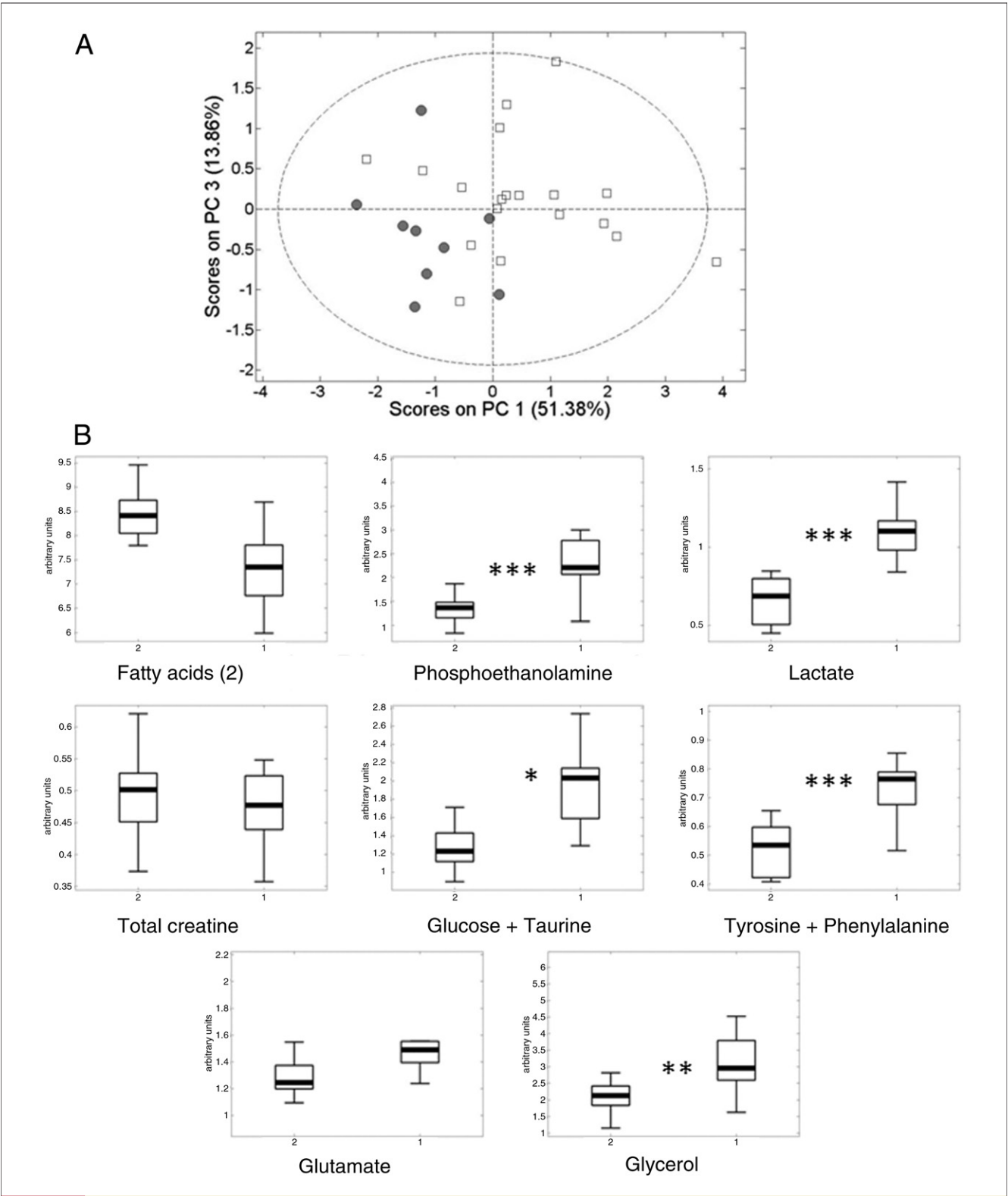


Figure 4 Metabolic Analysis in Controls and in Patients Undergoing Angioplasty-Induced Ischemia

Principal component analysis (PCA) and metabolic quantification of the blood samples obtained 10 min after the procedure in angiographic controls and in angioplasty-induced ischemia patients. **(A)** PCA score plot of blood serum nuclear magnetic resonance spectra in angiographic controls (**gray circles**) and in angioplasty-induced ischemia patients (**open squares**). **(B)** Box plots showing representative metabolite levels in blood serum of angiographic controls (box on the left) and of angioplasty-induced ischemia patients (box on the right) immediately after the procedure. The boxes and whiskers represent the same as in Figure 2. Levels are expressed as area of the metabolite of interest divided with respect total aliphatic spectral area. * $p < 0.02$; ** $p < 0.01$; *** $p < 0.001$.

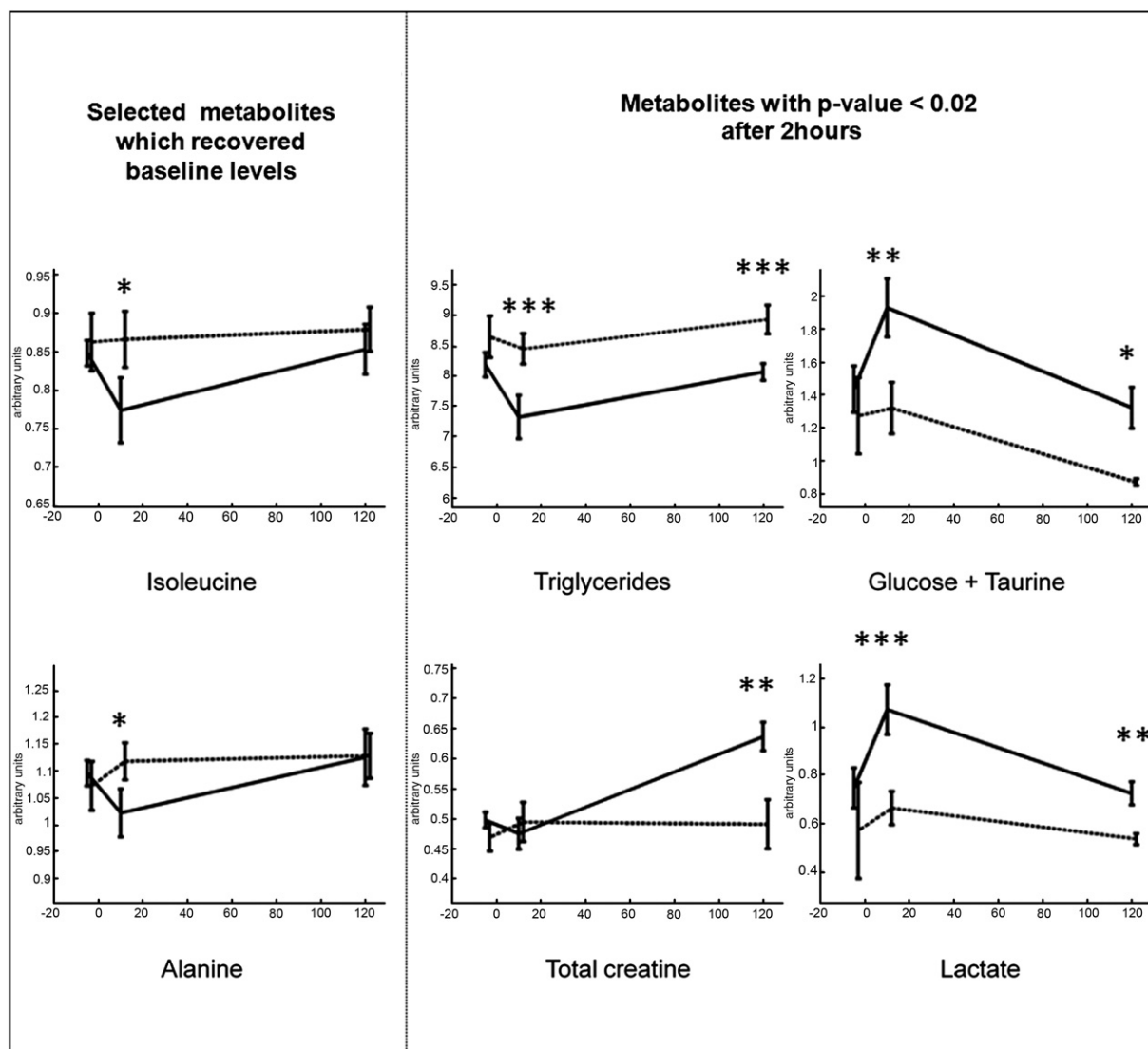


Figure 5 Time Changes of Selected Metabolites in Controls and in Angioplasty-Induced Ischemia Patients

Means and standard deviations of selected metabolites that recovered baseline levels and of metabolites with the highest statistical significance in angiographic controls (dashed lines) and in angioplasty-induced ischemia patients (solid lines) before and 10 and 120 min after the procedure. * $p < 0.05$; ** $p < 0.02$; *** $p < 0.001$.

sisted, though at lower intensity (Table 1). Most of these changes showed high statistical significance and reproducibility, with a relative error lower than 10%. Figure 2B shows box plots of metabolites selected on the basis of their statistical significance in relationship with ischemia. The swine MIS discrimination model based on those metabolites displaying the most significant changes accurately detected 97% of the swine samples tested.

Study in patients. Baseline characteristics of patients treated with percutaneous intervention in which MIS was induced and of controls in which angiography, but not angioplasty-induced ischemia, was performed are displayed in Online Table 2. Similarly to our experimental model, we first analyzed ischemia by using the recruited patients as

their own biological controls. The PCA score plot of human serum before and immediately after ischemia shows that MIS induced global metabolic changes (Fig. 3A) that were similar in nature and intensity to those observed in the swine model (Fig. 3B). Most of these changes were not observed in angiographic controls before and after angiography (Table 2).

To explore the potential diagnostic value of our analysis, we compared blood serum profiles obtained 10 min after the procedure in angiographic controls and in patients undergoing controlled ischemia. The PCA score plot of human serum comparing controls and patients 10 min after the procedure (Fig. 4A) shows significant differences, similar to those observed in patients before and immediately after

Table 3 Metabolite Levels in Patients With Spontaneous Chest Pain With and Without Final Diagnosis of Myocardial Ischemia

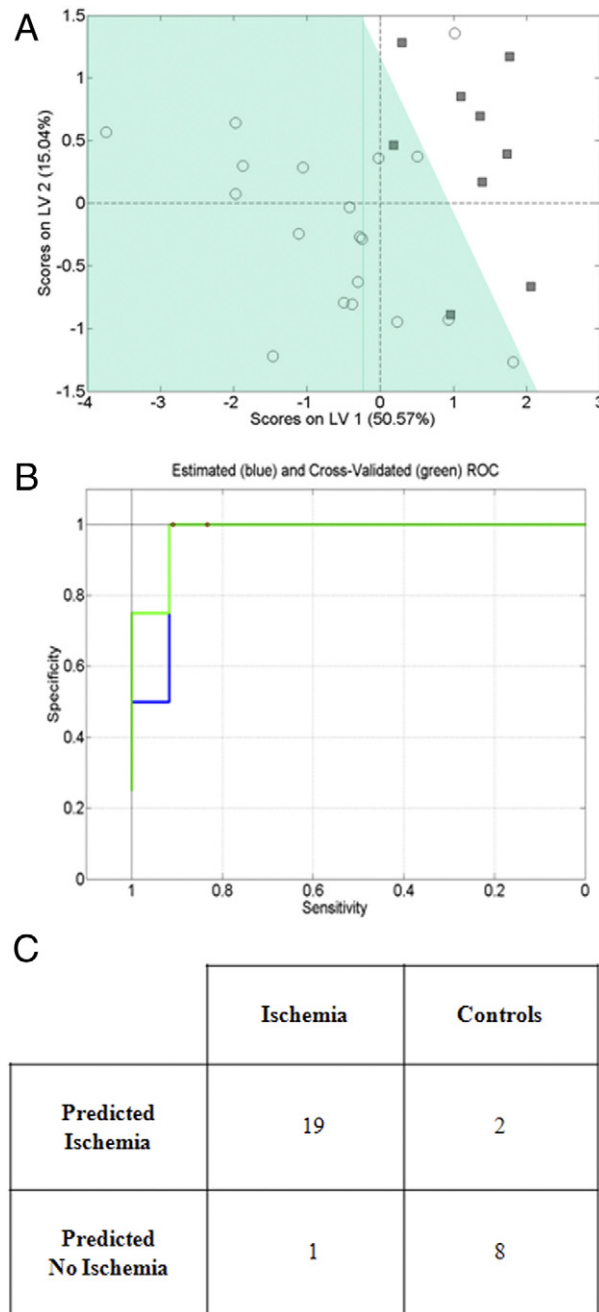
Metabolite Dominant in the Spectral Region	Mean Spectral Intensity (Arbitrary Units)		p Value
	Without Ischemia	With Ischemia	
Cholesterol	2.85 ± 0.55	2.67 ± 0.64	0.38
Triglycerides	8.55 ± 0.45	8.18 ± 0.75	0.18
Leucine	2.82 ± 0.24	2.65 ± 0.23	0.31
Isoleucine	0.89 ± 0.08	0.85 ± 0.07	0.78
Valine	0.72 ± 0.07	0.67 ± 0.07	0.64
3-hydroxybutyrate	1.90 ± 0.32	1.32 ± 0.26	0.03
FAs*	16.75 ± 2.63	14.84 ± 3.20	0.18
Alanine (overlapped)	1.19 ± 0.07	1.10 ± 0.09	0.16
FAs†	1.92 ± 0.25	1.63 ± 0.34	0.39
Acetate	1.82 ± 0.76	2.10 ± 1.17	0.98
Unsaturated FAs	2.70 ± 0.21	2.42 ± 0.40	0.53
Glycoproteins (acetyls)	2.20 ± 0.13	1.89 ± 0.25	0.04
FAs‡	1.86 ± 0.27	1.52 ± 0.37	0.53
Glutathione	1.31 ± 0.07	1.20 ± 0.16	0.10
Glutamate	0.60 ± 0.04	0.56 ± 0.08	0.25
Glutamine	0.69 ± 0.05	0.51 ± 0.10	0.04
Polyunsaturated FAs	1.95 ± 0.16	1.84 ± 0.33	0.95
Asparagine	0.58 ± 0.04	0.52 ± 0.06	0.10
Albumine lysyl§	0.75 ± 0.06	0.69 ± 0.07	0.06
Albumine lysyl§	0.26 ± 0.04	0.26 ± 0.06	0.45
Creatine	0.34 ± 0.06	0.34 ± 0.09	0.95
Choline	0.41 ± 0.08	0.42 ± 0.09	0.83
Phosphocholine	1.27 ± 0.16	1.32 ± 0.25	0.86
Glycerophosphocholine	0.52 ± 0.18	0.82 ± 0.25	0.70
Taurine	0.22 ± 0.07	0.35 ± 0.12	0.98
Proline	0.15 ± 0.05	0.24 ± 0.08	0.17
Glucose	1.28 ± 0.16	1.39 ± 0.26	0.34
Glycine	0.45 ± 0.07	0.55 ± 0.22	0.44
Glycerol	0.97 ± 0.45	1.49 ± 0.83	0.12
Glucose + taurine	0.91 ± 0.26	1.43 ± 0.51	0.11
Tyrosine + phenylalanine	1.37 ± 0.27	1.19 ± 0.34	0.37
Phosphoethanolamine	2.85 ± 0.55	2.67 ± 0.64	0.38
Lactate	8.55 ± 0.45	8.18 ± 0.75	0.18

Values are mean ± SD. *CH₃ groups in FAs. †CH₃ groups close to a CO group (CH₃-CO-) in FAs. ‡CH₃ groups close to a double bond (CH₃-CH=CH-) in FAs. §Different spectral positions for the same group in the same molecules.

FA = fatty acid.

ischemia (Fig. 3). Figure 4B shows the box plots of metabolites selected on the basis of their statistical significance in relationship with ischemia.

We monitored metabolite levels in human samples taken 2 h after the procedure to evaluate the time validity of our MIS metabolic profile. Total NMR visible FAs, acetate, and the amino acids leucine, isoleucine, and alanine recovered baseline levels 2 h after intervention in both patients and controls. In contrast, levels of triglycerides, glucose, lactate, glutamine, glycine, glycerol, and phospholipids were still significantly different between controls and patients after the same period of time. Creatine remained unaltered at 10 min but increased about 3-fold 2 h after intervention in patients. Figure 5 shows the intensity-versus-time curves


Figure 6 PLS-DA Model Performance for Discrimination Between Patients Undergoing Angioplasty-Induced Ischemia and Controls

Projection to latent structures for discriminant analysis (PLS-DA) score plot, receiver-operating characteristic (ROC) curve, and frequency table for discrimination between patients undergoing angioplasty-induced ischemia and controls on the basis of the PLS-DA model derived from blood samples obtained 10 min after the procedure. (A) Score plot of our PLS-DA model in angioplasty-induced ischemia patients (open circles) and angiographic controls (gray squares). (B) ROC curve for discrimination between patients undergoing angioplasty-induced ischemia and controls on the basis of our PLS-DA model (green = training data; blue = leave-one-out cross-validation). (C) Frequency table for discrimination between patients undergoing angioplasty-induced ischemia and controls on the basis of our PLS-DA model.

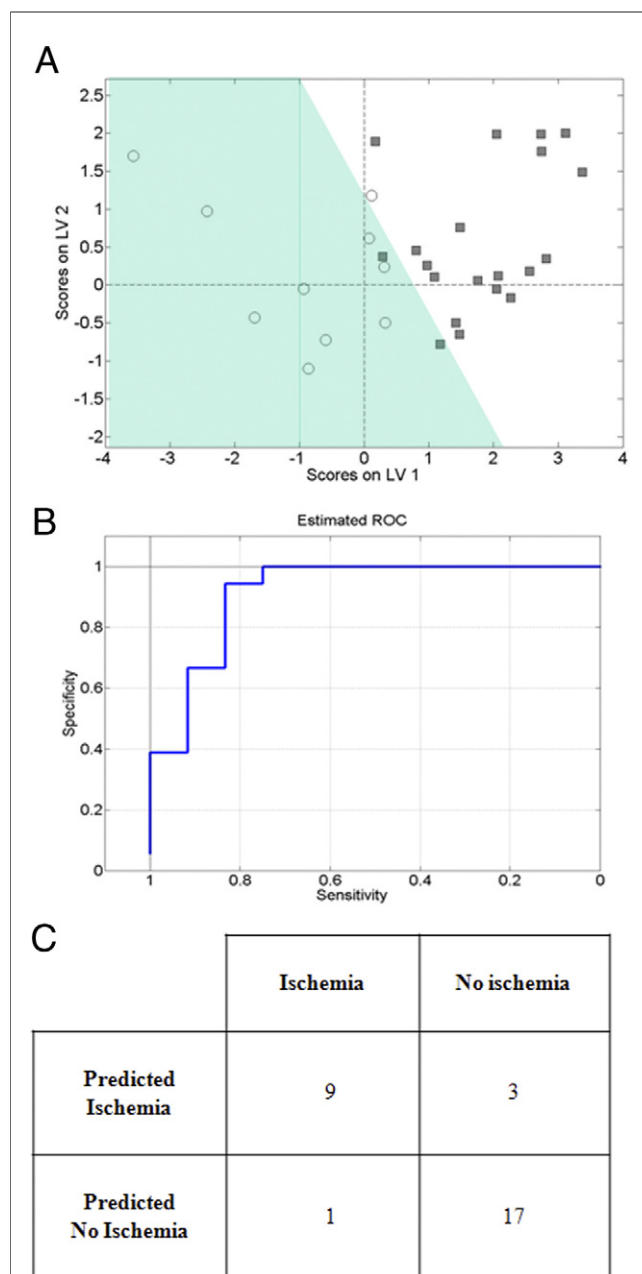


Figure 7

PLS-DA Model Performance for Discrimination Between Patients With Spontaneous Acute Chest Pain and With or Without a Final Diagnosis of Myocardial Ischemia

Projection to latent structures for discriminant analysis (PLS-DA) score plot, receiver-operating characteristic (ROC) curve, and frequency table for discrimination between patients with spontaneous acute chest pain and with or without final diagnosis of myocardial ischemia. (A) Score plot of our PLS-DA model in ischemic (open circles) and nonischemic (gray squares) spontaneous acute chest pain patients. (B) ROC curve for discrimination between ischemic and nonischemic spontaneous acute chest pain patients on the basis of our PLS-DA model. (C) Frequency table for discrimination between ischemic and nonischemic spontaneous acute chest pain patients on the basis of our PLS-DA model.

for selected metabolites that recovered baseline levels and for metabolites with the highest statistical significance ($p < 0.02$).

To explore the reliability of metabolic profiling for accurately distinguishing patients who underwent balloon-induced MIS from controls, we built and cross-validated a new human MIS discrimination model using the whole metabolic profile 10 min after ischemia (Fig. 6A). The PLS-DA model with 3 latent variables (loadings and scores for the 3 latent variables are represented and listed in Online Fig. 2 and Online Tables 4, 5, and 6) allowed clear discrimination immediately after ischemia, with a cross-validation error percent of 10% and a rate of false-negatives of 5%. The area under the curve of this model was 0.94 (95% confidence interval: 0.88 to 0.98) (Fig. 6B). Figure 6C contains the frequency table for detecting MIS using this PLS-DA model and cross-validation. The final cross-validated sensitivity and specificity of the model according to this table were 95% and 80%, respectively. The positive and negative predictive values were 90% and 88%, respectively.

Study group with spontaneous chest pain. The PLS-DA model defined in patients with angioplasty balloon-induced MIS was validated in patients with spontaneous chest pain evaluated in the emergency department. Baseline characteristics of patients with spontaneous chest pain with and without final diagnoses of MIS are displayed in Online Table 3. Our PLS-DA model accurately detected ischemic patients (Fig. 7A) with an error percent of 13% and a false-negative rate of 10%. The area under the curve of this model was 0.90 (95% confidence interval: 0.82 to 0.96) (Fig. 7B). The metabolic profile displayed a positive predictive value of 75% and a negative predictive value of 95%: of 18 cases in which the metabolic profile predicted the absence of MIS, only in 1 the diagnosis of MIS was established. Sensitivity was 90% and specificity 85% (Fig. 7C).

Discussion

The main finding of the present study is that, under highly controlled conditions of coronary flow restriction, immediate and striking changes in the metabolic profile of peripheral blood serum can be detected using NMR spectroscopy. **Translational nature of the approach.** In the first stage of this study, metabolomics in a swine model provided very reproducible, consistent, and robust markers of severe MIS. Afterward, this information was validated in human subjects. This 2-step approach has 2 main advantages. First, the study in an animal model allows a reproducible detection of markers of low sensitivity but potential high specificity in a severe ischemia scenario (5-min coronary occlusion in the absence of collateral vessels). Second, it reduces the number of human subjects needed for the validation study. Using this strategy, we identified those metabolites showing the most robust and statistically significant changes induced by ischemia. Then, we validated them in human subjects

undergoing controlled MIS in the setting of scheduled and clinically guided coronary angioplasty. All these metabolites established the metabolic biosignature of MIS.

The design of the present study allowed us to specifically focus on the effects of MIS on the blood serum metabolic profile, avoiding potential confounders encountered in previous series such as exercise-induced metabolic changes in peripheral large muscles (8) or myocardial necrosis (11).

Metabolic impact of MIS. The heart uses a diverse set of fuel substrates, including lactate, glucose, amino acids, ketones, and particularly free FAs (12,13). However, dramatic and immediate changes take place in cardiac and global metabolism as a consequence of insufficient blood flow to meet myocardial energy needs and the subsequent stress response (14). Among others, peroxisome proliferator-activated receptor alpha, peroxisome proliferator-activated receptor gamma coactivator 1-alpha, and estrogen-related receptor alpha transcription factors seem to be at the core of subsequent metabolic changes (15). We have shown that immediately after ischemia, there is a clear decrease in glucose uptake, a trend toward decreased FA extraction, and a clear switch from net lactate extraction to lactate release in the myocardium. Under acute ischemia, tricarboxylic acid cycle activity is compromised (16). Studies of failing human hearts have suggested down-regulation of enzymes related to FA oxidation and glucose metabolism (17). It is also well known that injury affects liver metabolism by the action of vasopressin, driving more acetyl coenzyme A toward the tricarboxylic acid cycle and less toward ketone body production (18,19). In addition, during hypoxia or ischemia, an increased reliance on anaerobic myocardial metabolism takes place, which increases the lactate release. Lactate must also be transported out of cardiac myocytes for maintenance of adenosine triphosphate levels. The overall result is an increase in circulating lactate after ischemia.

The initial pain-related catecholamine discharge acts on adipose tissue to mobilize FAs, which are released to blood to be preferentially oxidized by skeletal and cardiac muscle (20). The observed increase in glycerol suggests initial cycling of endogenous triacylglycerols in ischemia (21). Our data, however, revealed a reduction in the NMR signal of total FAs after ischemia. The NMR signal depends not only on a molecule's concentration but also on its physicochemical properties, which poses an advantage over other screening methods. Circulating free FAs are transported from adipose tissue to the periphery by binding to albumin, whose NMR signal is hidden in the spectral baseline. Therefore, the simultaneous increase in glycerol and decrease in NMR-visible FAs suggests increased production of free FAs by lipolysis in adipose tissue.

The metabolic alterations in myocardial energy production also affect other important metabolic pathways. Our results show significant reductions in choline-containing compounds. Changes in serum phospholipids have been

associated with silent MIS (22). Ischemia may induce a 50% reduction in the biosynthesis of phosphatidylcholine (23). We also have found a rise in phosphoethanolamine, a constituent of the inner leaflet of the cell membrane, with little presence on the surface of normal viable cells (24). Thus, this metabolite might be a very early marker of cell injury due to ischemia. Other changes include taurine and glutamine, which are amino acids known to be concentrated within cardiomyocytes (23). Alanine and glutamine follow opposite trends, as expected. Although the exact mechanisms for these alterations remain unknown, it could be speculated that the diseased heart may have less metabolic fitness to match substrate use on demand. Taurine has been described as a marker of disturbed cell integrity and lactate as a marker of compromised cell energy metabolism (25). Regarding the delayed increase in creatine, it could be explained by an increased ischemia-related transport of adenosine triphosphate between cytoplasm and the mitochondria of cardiomyocytes.

The metabolic changes observed in our study under highly controlled conditions of MIS are consistent with previous hypotheses developed from single-metabolite studies (18–25). Our results in swine and in patients show that these changes are detectable by NMR spectroscopic metabolomics in as little as a couple of drops (20 μ l) of peripheral blood serum (Online Fig. 2).

Clinical validation. The ultimate goal of biomarkers is to be helpful in correctly diagnosing patients in the clinical arena. We addressed this issue in the most challenging scenario, namely, consecutive patients with spontaneous acute chest pain presenting to the emergency department with normal troponin I values and nondiagnostic electrocardiographic results. Our metabolic biosignature showed high accuracy in discriminating those patients with and without final diagnoses of MIS. The performance of the constructed PLS-DA model for the discrimination of ischemia in patients with spontaneous chest pain was better than that achieved separately by any single metabolite (Online Fig. 3). In most cases, the final diagnosis was not achieved until after at least 12 h of thorough evaluation in the cardiology department.

Study limitations. Although an immense variety of factors can affect metabolism, in our controlled models of coronary ischemia in swine and humans, it is unlikely that the immediate and dramatic metabolic changes detected could be explained by other conditions apart from the transitory coronary flow interruption. Assessment of peripheral arterial and coronary sinus samples would likely have strengthened results; however, we developed a model with potential clinical application using a type of sample easy to obtain in all clinical settings. Undoubtedly, the clinical validation of the developed metabolic biosignature requires further studies including large series of patients with spontaneous chest pain.

Conclusions

Metabolomics, based on the model presented here, represents a robust, minimally invasive and cost-effective bioprofile (<\$13 per assay) for the detection of acute MIS with potential clinical application. Although metabolic profiling of acute MIS has been previously reported, this study reports, to our knowledge, the first metabolic biosignature of acute MIS developed under highly controlled models of coronary occlusion and tested in patients with spontaneous chest pain. Guided by judicious clinical assessment and a reasonable use of complementary explorations, it could be speculated that if our results are confirmed in larger series, the developed metabolic biosignature could be helpful in improving the diagnostic process in patients presenting to emergency departments for acute chest pain with no additional data on MIS.

Reprint requests and correspondence: Dr. Vicente Bodi, Cardiology Department, and/or Dr. Daniel Monleon, Fundacion de Investigacion, Hospital Clinico Universitario-INCLIVA, Universidad de Valencia, Blasco Ibanez 17, 46010 Valencia, Spain. E-mail: vicentbodi@hotmail.com and/or daniel.monleon@uv.es.

REFERENCES

1. Sanchis J, Bodi V, Nunez J, et al. New risk score for patients with acute chest pain, non-ST-segment deviation, and normal troponin concentrations: a comparison with the TIMI risk score. *J Am Coll Cardiol* 2005;46:443–9.
2. Morrow DA, de Lemos JA, Sabatine MS, Antman EM. The search for a biomarker of cardiac ischemia. *Clin Chem* 2003;49:537–9.
3. Kavsak PA, Wang X, Henderson M, Ko DT, Macrae AR, Jaffe AS. PAPP-A as a marker of increased long-term risk in patients with chest pain. *Clin Biochem* 2009;42:1012–8.
4. Bodi V, Sanchis J, Llacer A, et al. Multimarker risk strategy for predicting 1-month and 1-year major events in non-ST-elevation acute coronary syndromes. *Am Heart J* 2005;149:268–74.
5. Lewis GD, Asnani A, Gerszten RE. Application of metabolomics to cardiovascular biomarker and pathway discovery. *J Am Coll Cardiol* 2008;52:117–23.
6. Brindle JT, Antti H, Holmes E, et al. Rapid and noninvasive diagnosis of the presence and severity of coronary heart disease using ¹H-NMR-based metabolomics. *Nat Med* 2002;8:1439–44.
7. Sabatine MS, Liu E, Morrow DA, et al. Metabolomic identification of novel biomarkers of myocardial ischemia. *Circulation* 2005;112:3868–75.
8. Barba I, Jaimez-Auguet E, Rodriguez-Sinovas A, Garcia-Dorado D. ¹H NMR-based metabolomic identification of at-risk areas after myocardial infarction in swine. *MAGMA* 2007;20:265–71.
9. Heyndrickx GR, Millard RW, McRitchie RJ, Maroko PR, Vatner SF. Regional myocardial functional and electrophysiological alterations after brief coronary artery occlusion in conscious dogs. *J Clin Invest* 1975;56:978–85.
10. Bodi V, Sanchis J, Mainar L, et al. Right ventricular involvement in anterior myocardial infarction: a translational approach. *Cardiovasc Res* 2010;87:601–8.
11. Lewis G, Wei R, Liu E, et al. Metabolite profiling of blood from individuals undergoing planned myocardial infarction reveals early markers of myocardial injury. *J Clin Invest* 2008;118:3503–12.
12. Turer AT, Stevens RD, Bain JR, Muchlbauer, et al. Metabolomic profiling reveals distinct patterns of myocardial substrate use in humans with coronary artery disease or left ventricular dysfunction during surgical ischemia/reperfusion. *Circulation* 2009;119:1736–46.
13. Grainger DJ. Metabolic profiling in heart disease. *Heart Metab* 2006;32:22–5.
14. Stanley WC, Recchia FA, Lopaschuk GD. Myocardial substrate metabolism in the normal and failing heart. *Physiol Rev* 2005;85:1093–129.
15. Huss JM, Kelly DP. Nuclear receptor signaling and cardiac energetics. *Circ Res* 2004;95:568–78.
16. Liedtke AJ. Effects of coronary perfusion during myocardial hypoxia. Comparison of metabolic and hemodynamic events with global ischemia and hypoxemia. *J Thorac Cardiovasc Surg* 1976;71:726–35.
17. Sebastiani M, Giordano C, Nediani C, et al. Induction of mitochondrial biogenesis is a maladaptive mechanism in mitochondrial cardiomyopathies. *J Am Coll Cardiol* 2007;50:1362–9.
18. Williamson DH. Regulation of ketone body metabolism and the effects of injury. *Acta Chir Scand Suppl* 1981;507:22–9.
19. Sugden MC, Ball AJ, Ilic V, Williamson DH. Stimulation of [¹⁻¹⁴C]oleate oxidation to ¹⁴CO₂ in isolated rat hepatocytes by vasopressin: effects of Ca²⁺. *FEBS Lett* 1980;116:37–40.
20. Oliver MF. Control of free fatty acids during acute myocardial ischaemia. *Heart* 2010;96:1883–4.
21. Metzsch C, Liao Q, Steen S, Algotsson L. Myocardial glycerol release, arrhythmias and hemodynamic instability during regional ischemia-reperfusion in an open chest pig model. *Acta Anaesthesiol Scand* 2006;50:99–107.
22. Lin H, Zhang J, Gao P. Silent myocardial ischemia is associated with altered plasma phospholipids. *J Clin Lab Anal* 2009;23:45–50.
23. Choy PC, Chan M, Hatch G, Man RY. Phosphatidylcholine metabolism in ischemic and hypoxic hearts. *Mol Cell Biochem* 1992;116:53–8.
24. Emoto K, Toyama-Sorimachi N, Karasuyama H, et al. Exposure of phosphatidylethanolamine on the surface of apoptotic cells. *Exp Cell Res* 1997;232:430–4.
25. Zemgulis V, Ronquist G, Bjerner T, et al. Energy-related metabolites during and after induced myocardial infarction with special emphasis on the reperfusion injury after extracorporeal circulation. *Acta Physiol Scand* 2001;171:129–43.

Key Words: metabolomics ■ myocardial ischemia ■ nuclear magnetic resonance.

APPENDIX

For additional information about NMR data processing and the construction and validation of multivariate metabolomic models, additional statistical methods, and online tables and figures and their captions, please see the online version of this article.